Optical Feedback in Vertical-Cavity Surface-Emitting Lasers

A. Hsu, *Student Member, IEEE*, J.-F. P. Seurin, S. L. Chuang, *Fellow, IEEE*, and K. D. Choquette, *Member, IEEE*

***Abstract*—Optical feedback in a vertical-cavity surface-emitting laser due to a fiber facet of varying position is studied in experiment and theory. Measured spectra and light-current curves show periodic variations in resonant wavelength, threshold current, differential quantum efficiency, and output power as a function of fiber position. Theoretical results were obtained using a 2×2 vector propagation matrix method which models the laser and fiber in a single structure and shows good agreement with experimental results. A novel method for determining the linewidth enhancement factor α by analyzing the wavelength variation as a function of fiber position is presented and a value of $\alpha = 2.8$ was obtained.**

***Index Terms*—Linewidth enhancement factor, optical feedback, optical fiber, vertical-cavity surface-emitting laser.**

I. Introduction

In THE last decade, progress in the development of vertical-cavity surface-emitting lasers (VCSEL) has emerged to benefit fiber-optic communication systems due to excellent VCSEL performance characteristics and advantages in manufacturing and testing over their edge-emitting counterparts. VCSELs typically consist of a multi-quantum-well active region surrounded by top and bottom distributed Bragg reflectors (DBRs) which create the resonant cavity. The incorporation of oxide apertures for index-guided VCSEL design [1], [2] has allowed for lower threshold currents, higher powers, and single-mode operation.

When coupling laser light into glass optical fiber for optical communication systems, the presence of the fiber facet can create optical feedback in the laser cavity and change the operational characteristics of the laser. Optical feedback is generally considered to be detrimental to the performance of lasers because, under certain conditions, feedback can cause significant changes in spectrum [3], [4], power instabilities [5]–[7], relative intensity noise [8], [9], and polarization switching [10], [11].

An important and practical case to consider is that of fiber-induced feedback where the fiber facet is positioned to within less than two microns of the VCSEL. Heinrich *et al.* [12] showed experimentally that fiber feedback could have a significant effect on the spectrum and output power of multimode VCSELs. Law *et al.* [5] predicted power variations in VCSELs due to varying fiber facet position. There has been little work, however, in correlating experiment and theory for fiber-induced optical feedback in VCSELs. In this work, we experimentally and theoretically investigate the effects of optical feedback on a selectively-oxidized index-guided VCSEL operating in a single transverse mode. The device characteristics are studied as a function of fiber facet position. In addition, we present a method to estimate the linewidth enhancement factor of VCSEL's by studying the resonant wavelength variation as a function of fiber facet position. In Section II, we describe the effects of feedback on VCSEL operation and a 2×2 vector propagation matrix method used to model a combined VCSEL and fiber structure. In Section III, we present the experimental results and compare these results with theory in Section IV. We conclude with a summary of the results in Section V. We show that our theoretical results agree very well with the experimental results.

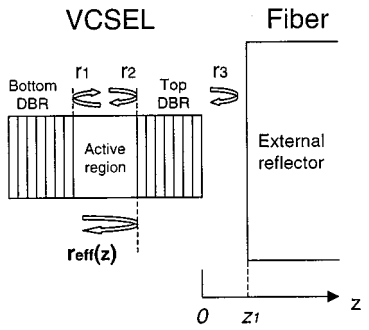

Fig. 1. Schematic of the VCSEL feedback model which consists of bottom and top DBRs with facet field reflectivities r_1 and r_2 and an external fiber reflector with reflectivity r_3. An effective reflectivity $r_{\rm eff}(z)$ is defined to take into account both r_2 and r_3. A linear change in position of the external reflector z results in a periodic change in magnitude and phase of the $r_{\rm eff}(z)$.

II. Theory and Modeling

We consider the case illustrated in Fig. 1 where the reflectivities are defined from the perspective of the active region of the VCSEL. The field reflectivity r_1 is the reflectivity from the bottom DBR, r_2 is the reflectivity from the top DBR, and r_3 is the reflectivity due to the fiber facet. An effective complex reflectivity $r_{\rm eff}$ with a phase $\phi_{\rm eff}$ can be defined for the top side which takes into account both r_2 and r_3. A linear change in the fiber position z results in a periodic variation in the magnitude and phase of $r_{\rm eff}$ with a period of half the resonant wavelength of the VCSEL. This periodic change in the $r_{\rm eff}$ leads to a change in a number of laser properties including

Manuscript received May 4, 2001.

A. Hsu, S. L. Chuang, and K. Choquette are with the Department of Electrical and Computer Engineering, the University of Illinois at Urbana-Champaign, Urbana, IL 61801 USA.

J.-F. P. Seurin was with the Department of Electrical and Computer Engineering, the University of Illinois at Urbana-Champaign, Urbana, IL 61801 USA. He is now with Princeton Optronics, Princeton, NJ 08543-8627 USA.

Publisher Item Identifier S 0018-9197(01)10041-2.

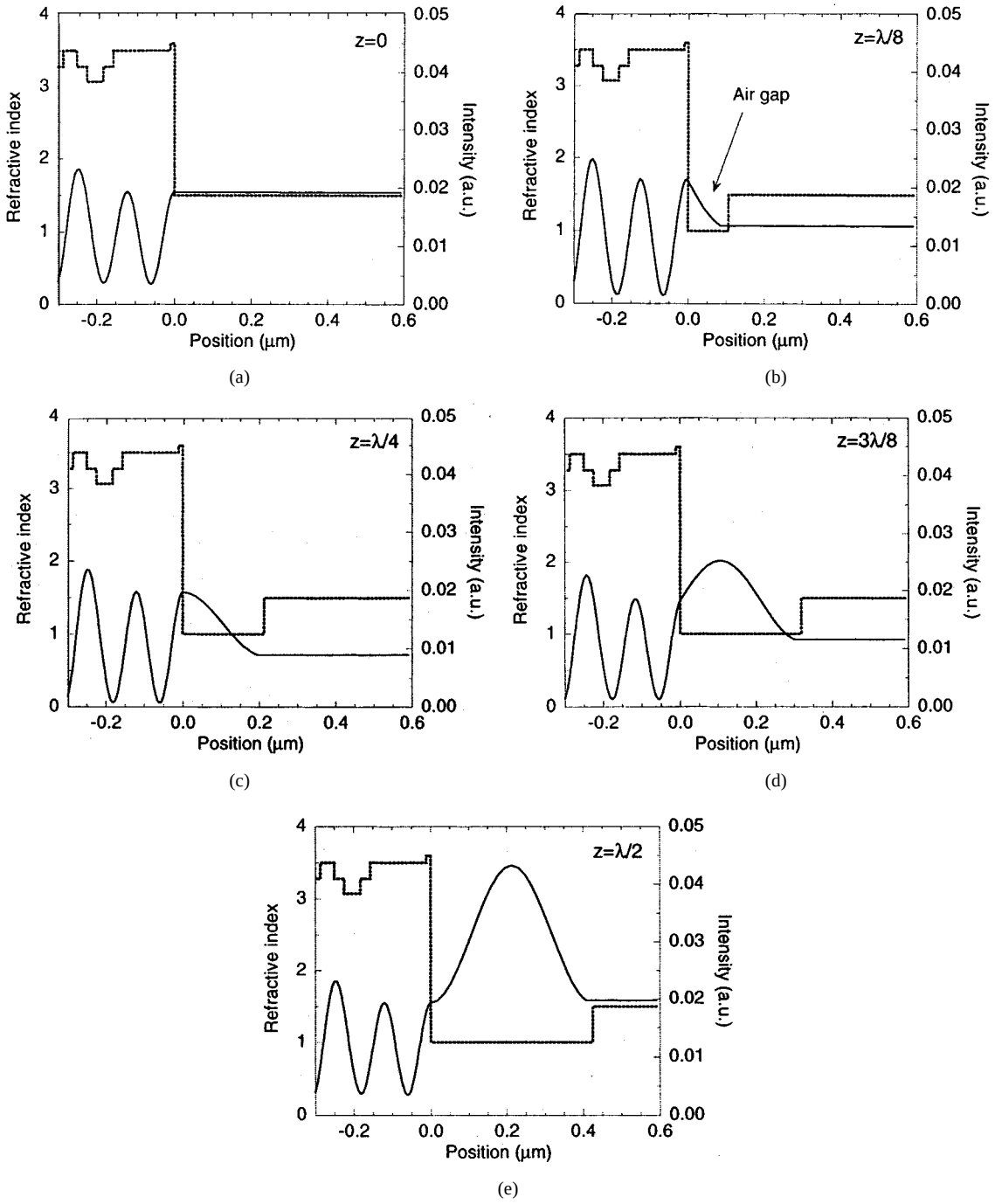

Fig. 2. Refractive index of VCSEL and fiber and intensity standing-wave patterns for: (a) $z = 0$; (b) $z = \lambda/8$; (c) $z = \lambda/4$; (d) $z = 3\lambda/8$; and (e) $z = \lambda/2$. The output intensity in the fiber varies periodically as a function of z.

threshold gain, resonant wavelength, differential quantum efficiency, and output power.

The mirror loss will decrease as a function of increasing r_{eff} and therefore the threshold gain and threshold current will also decrease. The resonant wavelength is affected by: 1) the change in ϕ_{eff} and 2) the gain-induced change in refractive index Δn through the linewidth enhancement factor as given by [13]

$$\Delta n = -\frac{\alpha\lambda}{4\pi}\,\Delta g. \tag{1}$$

The magnitude and phase of the wavelength variation with respect to the threshold gain depends on the value of the linewidth enhancement factor α. We can, therefore, determine α by experimentally measuring the change in resonant wavelength as a function of z and compare the results with theoretical simulations using different values of α.

A simplified Fabry–Pérot (FP) resonator feedback model is useful in explaining how optical feedback affects the properties of an edge-emitting semiconductor laser with well-defined facets [14]. Several groups have modeled feedback in VCSELs by defining effective cavity lengths and reflectivities for the VCSEL and using the FP model [5], [9], [7].

We take a more rigorous approach in modeling optical feedback in VCSELs by using a 2×2 vector propagation

matrix method [15], where the optical fiber is directly included in the modeled structure. The real and imaginary refractive index layers of the VCSEL and fiber were included in the simulated structure. The model calculates the plane-wave longitudinal standing wave and parameters for the VCSEL-fiber structure. The model also calculates the resonant wavelength and threshold gain for specific transverse modes.

The real part of the refractive index n for several upper layers of the top DBR ($3.0 \leq n \leq 3.5$), the glass optical fiber ($n = 1.5$), and air gap ($n = 1.0$) are plotted in Fig. 2 for $z = 0$, $\lambda/8$, $\lambda/4$, $3\lambda/8$, and $\lambda/2$, where z is the distance between the fiber facet and top DBR. To illustrate the effect of varying fiber facet position, the plane-wave longitudinal standing-wave patterns for the intensity are also plotted in Fig. 2. At $z = 0$, the standing wave is terminated at a peak which corresponds to maximum output power. At $z = \lambda/8$, the standing wave is not a resonant mode of the air cavity, resulting in a decrease in the output intensity and phase change. At $z = \lambda/4$, the output intensity reaches a minimum. At $z = 3\lambda/8$, the output intensity increases, and at $z = \lambda/2$, the standing wave is a resonant mode of the air cavity and the output intensity reaches the same value as at $z = 0$. It should be noted that feedback-dependent effects depend on the longitudinal structure of the VCSEL. Transverse structures such as the oxide apertures have virtually no effect on feedback.

III. Experiment

A. Device Structure

The device under study is a selectively-oxidized VCSEL grown in the AlGaAs–GaAs material system [16]. The active region has five quantum wells and is surrounded by barrier layers and top and bottom DBR layers. The top DBR has 23 pairs and the bottom DBR has 33.5 pairs. Selectively oxidized apertures which are 5×5 μm^2 in area were fabricated in the top and bottom DBR regions. The threshold current for this device is 4.4 mA. This particular device was chosen because it operates in a single mode up to 6 mA, corresponding to the fundamental mode (TEM_{00} or LP_{01} in fiber mode notation). This allows us to isolate feedback effects for a single mode and avoid more complex multimode interaction due to spatial hole burning [5].

B. Experimental Setup

The VCSEL was mounted on a thermoelectric cooler to keep the temperature constant at $T = 25$ °C. The light emission from the VCSEL was coupled into the cleaved facet of a 50-μm graded-index multimode fiber which was positioned less than 2-μm away from the top of the VCSEL. The fiber facet produces a power reflectivity of 4%. The fiber was mounted on a piezoelectric positioner and controller with a position resolution on the order of 10 nm. The other end of the fiber was connected to an optical spectrum analyzer to measure spectra and a power detector to measure light-current (*L–I*) curves at various fiber facet positions. For the spectral measurements, the VCSEL was current-biased at $I = 5.0$ mA.

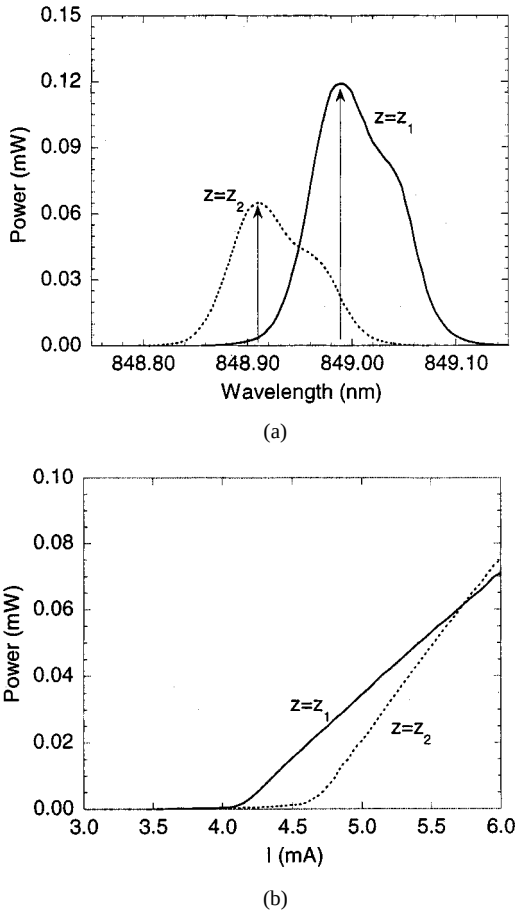

Fig. 3. (a) Measured spectra at arbitrary fiber facet positions $z = z_1$ and $z = z_2$ at $I = 5.0$ mA. (b) Measured *L–I* curves at $z = z_1$ and $z = z_2$. At $z = z_1$, $I_{th} = 4.1$ mA and $C_{LI}\eta_d = 0.027$ and for $z = z_2$, I_{th} increases to 4.5 mA and $C_{LI}\eta_d$ increases to 0.036.

C. Experimental Results

The properties of the spectra and *L–I* curves were observed to vary as a function of fiber facet position z as shown in Fig. 3 where the zero reference in z is arbitrary. The spectra for two fiber facet positions are shown in Fig. 3(a). At $z = z_1$, the resonant wavelength is $\lambda = 848.98$ nm and decreases to $\lambda = 848.91$ nm at $z = z_2$. The peak output power is also observed to decrease by about 50%. As shown in Fig. 3(b), the *L–I* curves show changes in threshold current and differential quantum efficiency for different fiber facet positions z. The differential quantum efficiency η_d is defined as

$$\eta_d = \frac{q}{\hbar\omega C_{LI}} \frac{dP}{dI} \tag{2}$$

where

- q electron charge;
- $\hbar\omega$ photon energy;
- C_{LI} experimental power-coupling efficiency for the *L–I* curve measurement;
- dP/dI measured slope of the *L–I* curve from I_{th} to $I = 6$ mA in W/A which is a function of fiber facet position z.

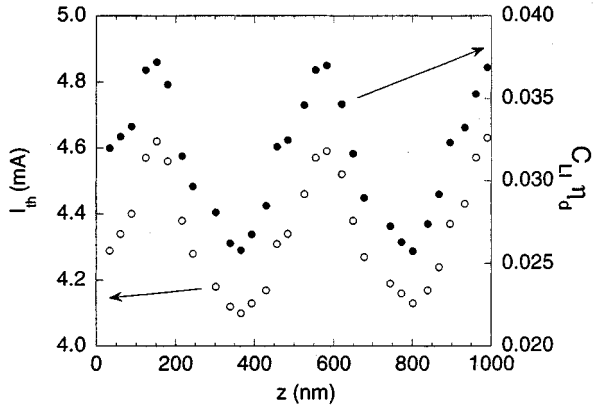

(a)

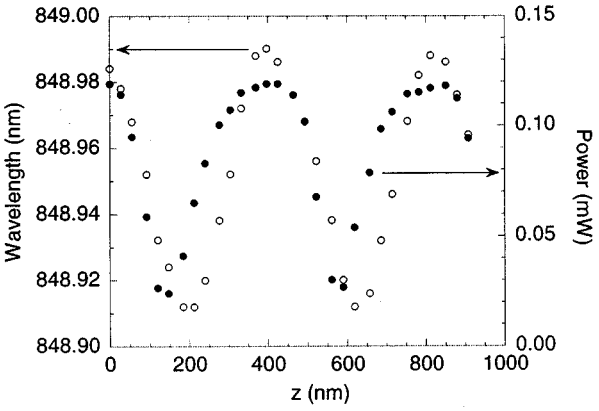

(b)

Fig. 4. (a) Measured threshold current and $C_{LI}\eta_d$ as a function fiber facet position z. (b) Measured resonant wavelength and peak fundamental mode power as a function of fiber facet position z.

In Fig. 3(b), at $z = z_1$, $I_{th} = 4.1$ mA, and $C_{LI}\eta_d = 0.027$, while for $z = z_2$, the I_{th} increases to about $I_{th} = 4.5$ mA and $C_{LI}\eta_d$ increases to 0.036.

Threshold current and $C_{LI}\eta_d$ values were extracted from the measured L–I curves over a 1-μm range of z and plotted in Fig. 4(a). The periodic behavior in threshold current and gain as expected from the feedback theory is observed, where the period corresponds to roughly half the resonant wavelength of 850 nm. Over this range, I_{th} varies from 4.1 to 4.6 mA, a variation of 11%, and $C_{LI}\eta_d$ varies by almost 40%. From the measured spectra, the resonant wavelength and peak fundamental mode power are plotted as a function of z in Fig. 4(b). The periodic behavior in resonant wavelength is observed with a variation of 0.08 nm and is shifted in phase with respect to the variation in threshold current. The output power varies significantly as a function of z. The position of the fiber facet clearly has a significant effect on the threshold current, differential quantum efficiency, and output power of the VCSEL.

IV. Comparison of Theory and Experiment

The model was used to calculate the resonant wavelength, threshold gain, differential quantum efficiency, and output power for the fundamental mode of the combined VCSEL-fiber structure.

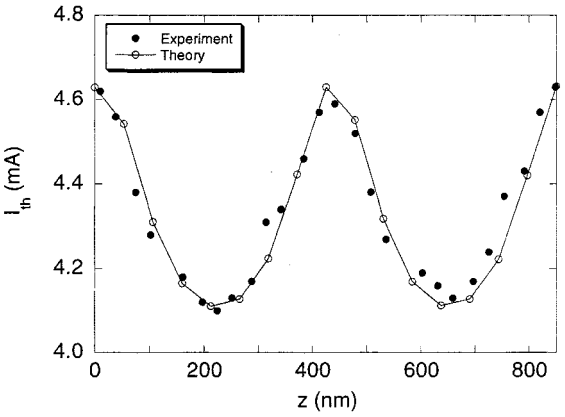

Fig. 5. Experimental and theoretical threshold current I_{th} as a function of fiber facet position z. The experimental position axis has an arbitrary reference and is aligned to the simulation position axis. The discrete simulation points are connected with lines to guide the eye.

A. Threshold Current

For a quantum-well laser, the threshold current density can be written as [13]

$$J_{th} = \frac{J_o}{\eta_i} \exp\left(\frac{g_{th}}{g_o} - 1\right) \tag{3}$$

where

J_o, g_o threshold current density and peak gain constants, respectively, used in the empirical logarithmic formula for the peak gain-current density relation;

η_i internal quantum efficiency;

g_{th} threshold gain.

We can define J_{th} and g_{th} as

$$J_{th} = J_{th,o} + \Delta J_{th} \tag{4}$$

$$g_{th} = g_{th,o} + \Delta g_{th} \tag{5}$$

where $J_{th,o}$ is a steady-state component and ΔJ_{th} is a varying component which is a function of the fiber facet position z and similarly for g_{th}. By substituting (4) and (5) into (3) and solving for the steady-state and varying threshold density components explicitly, we can write the threshold current density as

$$J_{th} = J_{th,o} \exp\left(\frac{\Delta g_{th}}{g_o}\right) \tag{6}$$

and similarly for the threshold current

$$I_{th} = I_{th,o} \exp\left(\frac{\Delta g_{th}}{g_o}\right) \tag{7}$$

where $\Delta g_{th} = g_{th}(z) - g_{th,o}$ and $g_{th}(z)$ is given by the model. Using (7), we can fit the experimental data by setting $g_{th,o}$ to the $g_{th}(z = 0)$ value, $g_{th,o} = 1650$ cm^{-1}, which is the maximum value over the fiber position range. We set $I_{th,o}$ to the corresponding maximum measured value of $I_{th,o} = 4.62$ mA. Using a reasonable value of $g_o = 3300$ cm^{-1} [14], we obtain theoretical results for I_{th} and compare them with experiment as shown in Fig. 5. The experimental position axis has an arbitrary

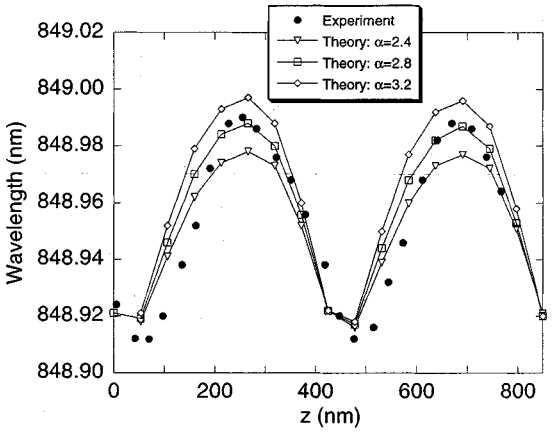

Fig. 6. Experimental and theoretical resonant wavelength for $\alpha = 2.4$, 2.8, and 3.2 as a function of fiber facet position z. The $\alpha = 2.8$ gives the best fit in terms of the magnitude and phase of the fit. The error in determining α is estimated at ± 0.2.

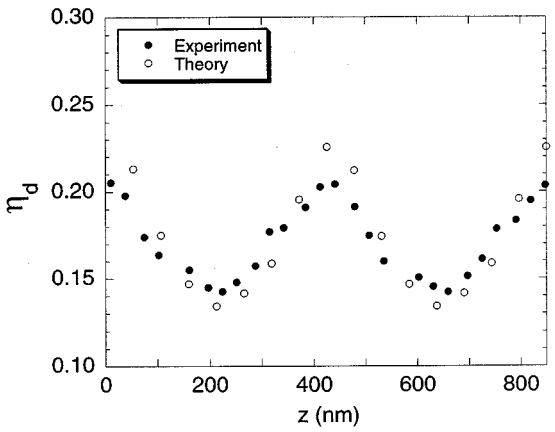

Fig. 7. Experimental and theoretical differential quantum efficiency η_d as a function of fiber facet position z.

reference point since the exact position of the fiber facet was not known during measurements and is aligned to the simulation axis such that the maximum experimental I_{th} occurs at the same position as the maximum theoretical g_{th}. The same position offset is used in the all subsequent comparisons between experiment and theory. The discrete simulation points are connected with lines to guide the eye. The experimental and theoretical I_{th} are in good agreement, considering that the only one fitting parameter g_o was used.

B. Resonant Wavelength

Because the model is an optical solver, it will simulate the variation in the resonant wavelength due to the $\phi_{\text{eff}}(\text{z})$ contribution only. However, the wavelength shift due to the gain-induced change in refractive index Δn as given by (1) is also included in the following way. We assume that a change in threshold gain g_{th} from the $\text{z} = 0$ reference is equivalent to a change in gain Δg in (1), and calculate the resulting Δn for a given value for α. This Δn is added to the real part of the refractive index of the quantum wells in the modeled structure and the simulation is run again to determine the total wavelength shift. The threshold gain g_{th} changed by less than 1% between the two simulations so iterative simulations between the threshold gain and resonant wavelength were not necessary. Shown in Fig. 6 is the experimental data for resonant wavelength as a function of z and the simulation results for $\alpha = 2.4$, 2.8, and 3.2. The result for $\alpha = 2.8$ clearly gives the best fit in terms of magnitude and phase with the experimental data. This value falls within the values of other reported results for the measured linewidth enhancement factor of VCSELs which range from 2.3 to 3.7 [17]–[20]. Using this method, we estimate an error of ± 0.2 in determining α. From (2), we can see that for $\alpha = 2.8$, the second wavelength shift contribution leads to an increase of the magnitude of the wavelength shift by a factor of three over the phase-shift contribution alone. The overall wavelength shift of 0.08 nm, however, remains relatively small. We note that heating in the active region will also induce changes in the refractive index which will depend on fiber position, but we found this effect to be negligible for the low current bias used here.

C. Differential Quantum Efficiency

The differential quantum efficiency η_d is an important parameter of a semiconductor laser which determines the output power. The effect of fiber facet position z on differential quantum efficiency is approximately given by [14]

$$\eta_d(z) = F(z)\eta_i \frac{\alpha_m(z)}{\Gamma g_{th}(z)} \tag{8}$$

where

η_i internal quantum efficiency;
$\alpha_m(z)$ mirror loss;
Γ optical confinement factor;

and

$$F(z) = \frac{T_{\text{eff}}(z)}{(1 - R_{\text{eff}}(z)) + \sqrt{\dfrac{R_{\text{eff}}(z)}{R_1}}\,(1 - R_1)} \tag{9}$$

where $R_{\text{eff}}(z)$ and $T_{\text{eff}}(z)$ are the effective power reflectivity and transmittivity from the top DBR and fiber and R_1 is the power reflectivity from the bottom DBR. $F(z)$ is the fraction of the total power out of the top facet. In calculating $\eta_d(z)$ from (8), we take values for $g_{th}(z)$, $T_{\text{eff}}(z)$, and $R_{\text{eff}}(z)$, L, and Γ from the simulation results and choose a value for η_i of 0.9. For the measured η_d in (2), we use C_{LI} as a constant fitting parameter over the small distance range and choose $C_{LI} = 0.18$. Fig. 7 shows the measured and calculated η_d as a function of z and the results show good agreement. These results show that varying fiber facet position can produce a significant variation of 40% in the differential quantum efficiency. Because of the low transmittivities from the DBR facets, feedback-induced changes in R_{eff} of the top facet results in large changes in T_{eff} on the order of 50% in the simulations. Therefore, the F term dominates the periodic behavior in η_d.

D. Output Power

Because the differential quantum efficiency and threshold gain vary periodically with fiber facet position, the output

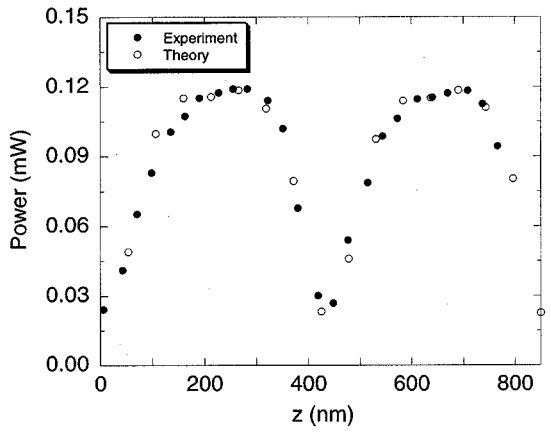

Fig. 8. Experimental (open circles) and theoretical (closed circles) output power of the fundamental mode as a function of fiber facet position z.

power is also expected to vary. The output power can be written as

$$P_{out,\,th}(z) = \eta_d(z)\,\frac{\hbar\omega}{q}\,(I - I_{th}(z)). \tag{10}$$

From the previous sections, $\eta_d(z)$ and $I_{th}(z)$ have been calculated, and I is the known experimental value of 5.0 mA. Fig. 8 shows the theoretical results and the measured results from Fig. 3(b). The agreement between theory and experiment is very good.

V. Conclusion

In summary, we have presented an experimental and theoretical study of fiber-induced optical feedback in an index-guided VCSEL. We show that a 2×2 vector propagation matrix method model correctly predicts the effects of the fiber-induced feedback on threshold gain, resonant wavelength, differential quantum efficiency, and output power for the VCSEL with good agreement between theory and experiment. In fitting the measured resonant wavelength variation behavior with theory, we have developed a method to determine the linewidth enhancement factor in VCSELs which is applicable to semiconductor lasers in general. A value of $\alpha = 2.8$ with an estimated error of ± 0.2 was determined for our VCSEL.

Acknowledgment

The authors would like to thank A. A. Allerman and K. M. Geib at Sandia National Laboratories for the growth and fabrication of the VCSEL device used in this work.

References

[1] D. L. Huffacker, D. G. Deppe, K. Kumar, and T. J. Rogers, "Native-oxide confined ring contact for low threshold vertical-cavity lasers," *Appl. Phys. Lett.*, vol. 65, pp. 97–99, 1994.

[2] K. D. Choquette, R. P. Schneider, K. L. Lear, and K. M. Geib, "Low threshold voltage vertical-cavity lasers fabricated by selective oxidation," *Electron. Lett.*, vol. 30, pp. 2043–2044, 1994.

[3] Y. C. Chung and Y. H. Lee, "Spectral characteristics of vertical-cavity surface-emitting lasers with external optical feedback," *IEEE Photon. Technol. Lett.*, vol. 3, pp. 597–599, 1991.

[4] S. Jiang, M. Dagenais, and R. A. Morgan, "Spectral characteristics of vertical-cavity surface-emitting lasers with strong external optical feedback," *IEEE Photon. Technol. Lett.*, vol. 7, pp. 739–741, 1995.

[5] J. Y. Law and G. P. Agrawal, "Effects of optical feedback on static and dynamic characteristics of vertical-cavity surface-emitting lasers," *IEEE J. Select. Topics Quantum Electron.*, vol. 3, pp. 353–358, 1997.

[6] P. S. Spencer, C. R. Mirasso, and K. A. Shore, "Effect of strong optical feedback on vertical-cavity surface-emitting lasers," *IEEE Photon. Technol. Lett.*, vol. 10, pp. 191–193, 1998.

[7] S. F. Yu, "Nonlinear dynamics of vertical-cavity surface-emitting lasers," *IEEE J. Quantum Electron.*, vol. 35, pp. 332–341, 1999.

[8] K. P. Ho, J. D. Walker, and J. M. Kahn, "External optical feedback effects on intensity noise of vertical-cavity surface-emitting lasers," *IEEE Photon. Technol. Lett.*, vol. 5, pp. 892–895, 1993.

[9] L. N. Langely and K. A. Shore, "Effect of optical feedback on the noise properties of vertical cavity surface emitting lasers," *IEE Proc. Optoelectron.*, vol. 144, pp. 34–38, 1997.

[10] A. Valle, L. Pesquera, and K. A. Shore, "Polarization selection and sensitivity of external cavity vertical-cavity surface-emitting laser diodes," *IEEE Photon. Technol. Lett.*, vol. 10, pp. 639–641, 1998.

[11] P. Besnard, M. L. Chares, G. Stephan, and F. Robert, "Switching between polarized modes of a vertical-cavity surface-emitting laser by isotropic optical feedback," *J. Opt. Soc. Amer. B*, vol. 16, pp. 1059–1063, 1999.

[12] J. Heinrich, E. Zeeb, and K. J. Ebeling, "Transverse modes under external feedback and fiber coupling efficiencies of VCSEL's," *IEEE Photon. Technol. Lett.*, vol. 10, pp. 1365–1367, 1998.

[13] S. L. Chuang, *Physics of Optoelectronics Devices*. New York: Wiley, 1995.

[14] L. A. Coldren and S. W. Corzine, *Diode Lasers and Photonic Integrated Circuits*. New York: Wiley, 1995.

[15] J.-F. Seurin and S. L. Chuang, "Vector numerical mode-matching model for VCSELs,", to be published.

[16] K. D. Choquette, W. W. Chow, G. R. Hadley, H. Q. Hou, and K. M. Geib, "Scalability of small-aperture selectively oxidized vertical-cavity lasers," *Appl. Phys. Lett.*, vol. 70, pp. 823–825, 1997.

[17] B. Moller, E. Zeeb, U. Fiedler, T. Hackbarth, and K. J. Ebeling, "Linewidth enhancement factor of vertical-cavity surface-emitting laser diodes," *IEEE Photon. Technol. Lett.*, vol. 6, pp. 921–923, 1994.

[18] D. Kuksenkov, S. Feld, C. Wilmsen, H. Temkin, S. Swirhun, and R. Leibenguth, "Linewidth and α-factor in AlGaAs/GaAs vertical cavity surface emitting lasers," *Appl. Phys. Lett.*, vol. 66, pp. 277–279, 1995.

[19] R. Jin, D. Boggavarapu, G. Khitrova, H. M. Gibbs, Y. Z. Hu, and S. W. Koch, "Linewidth bradening factor of a microcavity semiconductor laser," *Appl. Phys. Lett.*, vol. 61, pp. 1883–1885, 1992.

[20] D. Kuksenkov, H. Temkin, and S. Swirhun, "Frequency modulation characteristics of gain-guided AlGaAs/GaAs vertical-cavity surface-emitting lasers," *Appl. Phys. Lett.*, vol. 66, pp. 3239–3241, 1995.

A. Hsu (S'01) received the B.S. and M.S. degrees in electrical engineering from the University of Illinois at Urbana-Champaign in 1996 and 1998, respectively, where he is currently working toward the Ph.D. degree.

His research interests include the design, characterization, and modeling of vertical-cavity surface-emitting lasers, distributed feedback lasers, integrated laser-modulators devices, and tunable lasers. His research has been in the areas of optoelectronics and optics at IBM, Rochester, MN, NTT Basic Research Laboratories, Atsugi, Japan, and Bell Laboratories, Murray Hill, NJ.

J.-F. P. Seurin was born in Rodez, France, in 1971. He received the Dipl.Ing. degree in electrical engineering from Ecole Nationale Supérieure des Télécommunications, (ENST), Paris, France, in 1995, and the M.S. and Ph.D. degrees in electrical engineering from the University of Illinois at Urbana-Champaign in 1996 and 2001, respectively. His doctoral research focused on the theoretical and experimental investigation of index-guided vertical-cavity surface-emitting lasers for optical communication applications.

His main research interests are in the fields of electromagnetics, numerical modeling, optoelectronics, and fiber-optics. He is currently with Princeton Optronics, Mercerville, NJ, a manufacturer of long-wavelength optoelectronic devices .

S. L. Chuang (S'78–M'82–SM'88–F'97) received the B.S. degree in electrical engineering from National Taiwan University, Taiwan, R.O.C., in 1976, and the M.S., E.E., and Ph.D. degrees in electrical engineering from the Massachusetts Institute of Technology, Cambridge, in 1980, 1981, and 1983, respectively.

In 1983, he joined the Department of Electrical and Computer Engineering, University of Illinois at Urbana-Champaign, where he is currently a Professor. He was a Resident Visitor at AT&T Bell Laboratories, Holmdel, NJ, in 1989, and a Consultant at Bellcore and Polaroid in 1991. He was a Senior Visiting Professor (Sabbatical Chair) at the SONY Research Center in 1995 and an Invited Professor at NTT Basic Research Laboratories, Atsugi, Japanin 1997. He was also a visitor at NASA Ames Research Center and Fujitsu Research Laboratories during the summer of 1999 and 2000, respectively. He is conducting research on strained quantum-well semiconductor lasers, modulators, infrared detectors, fiber-optic sensors, and optical networks. He is the author of *Physics of Optoelectronic Devices* (New York: Wiley, 1995). He has published around 200 journal and conference papers and given many invited talks at conferences and institutions. He has been cited many times for Excellence in Teaching at the University of Illinois.

Dr. Chuang is an Associate Editor of the IEEE JOURNAL OF QUANTUM ELECTRONICS. He was a Feature Editor for a Special Issue on Terahertz Generation, Physics and Applications of the *Journal of Optical Society of America B* in 1994. He is a Fellow of the Optical Society of America, and a member of the American Physical Society. He received the Andersen Consulting Award for Excellence in Advising in 1994 and was selected as an Associate at the Center for Advanced Study at the University of Illinois in 1995. He was also awarded a Fellowship from the Japan Society for the Promotion of Science to visit the University of Tokyo in 1996.

K. D. Choquette (M'89) received the B.S. degrees in engineering physics and applied mathematics from the University of Colorado at Boulder in 1984 and the M.S. and Ph.D. degrees in materials science from the University of Wisconsin–Madison in 1985 and 1990, respectively.

From 1990 to 1992, he held a postdoctoral position at AT&T Bell Laboratories, Murray Hill, NJ. In 1993, he joined Sandia National Laboratories, Albuquerque, NM. In 2000, he joined the Electrical and Computer Engineering Department, University of Illinois at Urbana-Champaign. His research interests include the design, fabrication, and characterization of vertical-cavity surface emitting lasers (VCSELs) and other optoelectronic devices. He has developed VCSELs emitting at wavelengths between 650–1300 nm, as well as the monolithic selectively oxidized VCSEL. His research interests also extend to novel fabrication technologies, hybrid integration techniques, and nano-fabrication processes. He has authored over 100 publications and two book chapters, and has presented numerous invited talks and tutorials on VCSELs.

Dr. Choquette is a IEEE/LEOS Distinguished Lecturer (2000–2002). He is an Associate Editor of the IEEE JOURNAL OF QUANTUM ELECTRONICS and is a member of the IEEE Lasers and Electro-Optics Society (LEOS) and the Optical Society of America (OSA).